

# Modeling and Experimental Verification in S+C+L+U Quadrable-Band WDM Transmission System using C+L-Band Transceivers and Wavelength Converters

Hide Nobu Muranaka<sup>1</sup>, Tomoyuki Kato<sup>1</sup>, Tomohiro Yamauchi<sup>1</sup>, Hiroyuki Irie<sup>1</sup>, Hiroki Ooi<sup>1</sup>, Yu Tanaka<sup>1</sup>, Shimpei Shimizu<sup>2</sup>, Takayuki Kobayashi<sup>2</sup>, Takushi Kazama<sup>2,3</sup>, Masashi Abe<sup>3</sup>, Takeshi Umeki<sup>2,3</sup>, Yutaka Miyamoto<sup>2</sup>, and Takeshi Hoshida<sup>1</sup>

<sup>1</sup>Fujitsu Limited, 4-1-1 Kamikodanaka, Nakahara-ku, Kawasaki, Kanagawa, Japan

<sup>2</sup>NTT Network Innovation Laboratories, 1-1 Hikari-no-oka, Yokosuka, Kanagawa, Japan

<sup>3</sup>NTT Device Technology Laboratories, 3-1 Morinosato Wakamiya, Atsugi, Kanagawa, Japan

Author E-mail address: muranaka.hide@fujitsu.com

**Abstract:** We experimentally verify wideband WDM transmission modeling in over 17-THz S+C+L+U quadrable-band transmission using PPLN-based wavelength converters. We confirmed within 3.3-dB errors between modeling after 80-km SSMF transmission of DP-16QAM and DP-QPSK signal. © 2024 The Author(s)

## 1. Introduction

Multi-band WDM transmission is one of the attractive solutions in recent years to the increasing communication capacity. In multi-band WDM transmission demonstrations, S+C+L triple-band systems have been mainly reported [1-3]. However, more recently, more than quadrable-band WDM transmission have been demonstrated, in which some O-, E-, S- and U- band are added to C+L-band [4-7]. On the other hand, for over 100-nm signal bandwidth transmission, optimization of each channel power is one of the major challenges in wide-band WDM systems due to signal power transfer caused by inter-channel stimulated Raman scattering (ISRS) effect. As a technique for improving transmission characteristics by optimizing the power of each channel, ISRS Gaussian noise (ISRS GN) closed-form models to estimate the amplified spontaneous emission (ASE) noise and nonlinear interference (NL) generation has been mainly used [8-10]. However, these modeling-based techniques have been validated experimentally C+L-band [9] and S+C+L-band transmission [3,10], but more than 4-band WDM transmission has not been validated experimentally yet.

In this paper, we first experimentally validate S+C+L+U quadrable-band WDM transmission modeling. S- and U-band WDM signal was generated by C-band ASE source, wavelength selective switch (WSS) and two types of PPLN-based wavelength converters with different pump wavelengths [11,12]. The generalized signal-to-noise ratio (GSNR) is estimated from linear SNR\_ASE and nonlinear SNR\_NL in each device and transmission line used in transmission experiment. GSNR can be converted to GOSNR depending on the type of signal used for transmission. On the other hand, based on the curve of GOSNR versus pre-FEC BER of back-to-back in the transceiver, the calculated GOSNR based on GSNR and converted GOSNR from measured pre-FEC BER can be compared. 80-km G. 652.D transmission was carried out under quasi-linear to nonlinear propagation conditions, and the error between measured and estimated pre-FEC BER was less than 3.3-dB.

## 2. Modeling of WDM transmission system using wavelength converters

Figure 1 shows a simulation model of single-span quadrable-band WDM transmission using wavelength converters (WC). In this model, C-band WDM signal is converted to S-band and U-band WDM signals by WCs, and then converted back to C-band after passing through the transmission line. As described later, due to the limitation of

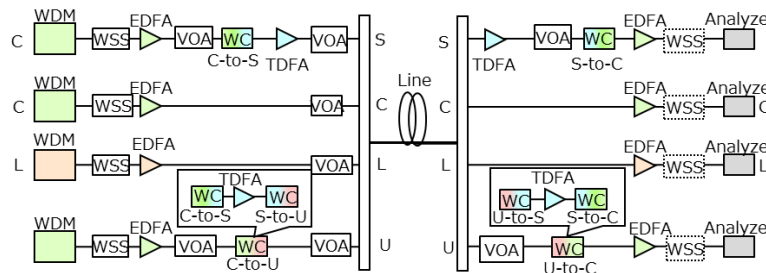


Fig. 1 Quadrable-band WDM transmission model

pump frequency of WC in the experiment, U-band WDM signal is generated by using twice wavelength conversion of converting C-band into S-band and converting S-band into U-band. S-band WDM signal converted by WC is amplified by Thulium-doped fiber amplifier (TDFA), while U-band WDM signal also converted by WC is transmitted without amplification. Since pre-FEC BER is an indicator of transmission performance obtained from our used transceiver, the correspondence between GSNR and pre-FEC BER is treated as follows. GSNR is obtained from the reciprocal sum of SNR\_ASE and SNR\_NL [8]. In this model, SNR\_ASE is obtained from the reciprocal sum of SNR of EDFA for C- and L-band, TDFA for S-band, and WC for S- and U-band. SNR\_NL is obtained from the reciprocal sum of WC and transmission line for each band. Each WC sets SNR\_NL individually according to the input power to the WC because the output power of the idler light generally changes nonlinearly when the input power of the signal exceeds a certain region. GSNR is converted to the GOSNR according to the Baudrate of each signal type as following formula,

$$\text{GOSNR} = \text{GSNR} + 10 \cdot \log_{10} (\text{Baudrate}/12.5\text{GHz}) \quad (1)$$

We also measure a back-to-back GOSNR versus pre-FEC BER curve of the transceiver and converted GOSNR is obtained from the measured pre-FEC BER based on this curve. Then, the converted GOSNR from measured pre-FEC BER and calculated GOSNR from the above equation are compared.

### 3. Experiments and Verification modeling

Experimental setup of S+C+L+U quadrable-band WDM transmission is shown in Fig.2. 400-Gb/s DP-16QAM C+L-band real-time transceivers were used as C+L-band test output channels, and 200-Gb/s DP-QPSK C-band real-time transceiver was converted into S- and U-band test output channels by PPLN-based WCs. By combining ASE light sources, WSSs, and WCs, WDM signals with 87.5-GHz spaced 60-GHz signal bandwidth were generated for 55-channels in 191.344 -196.156 THz range for C-band, 58-channels in 185.831 - 190.906 THz range for L-band, 51-channels in the 196.594 - 201.056 THz range for S-band, and 42-channels in 180.844 - 184.606 THz range for U-band. WC1 and WC4 are used for conversion between C-band and S-band (fundamental pump frequency of  $\nu_F = 196.200$  THz), and are described in detail in [11]. Although WC2 and WC3 are suitable for conversion between C-band and L-band (fundamental pump frequency of  $\nu_F = 190.600$  THz), temperature tuning of PPLN is performed to achieve wide-band wavelength conversion between S-band and U-band [12]. Using WDM signal whose signal bandwidth was reduced to 40-GHz, the input and output spectra and conversion efficiency (CE) of each WC are shown in Fig. 2 (a)-(d). The input power was +10 dBm for WC1 and WC4, +22 dBm for WC2, and -10 dBm for WC3. The inter-channel deviations are ranged from 0.7 to -3.3 dB for WC1, -5.4 to -12.1 dB for WC2, -1.4 to -8.4 dB for WC3, and -1.3 to -5.5 dB for WC4. WDM signal combining S-, C-, L-, and U- band was launched into the G. 652.D 80-km SSMF whose wavelength dependence of the transmission loss was shown in Fig. 2 (e) and was again divided into each band after 80-km transmission. S-band WDM signals passed through the transmission line and converted from U-band by WC3 are selected by an optical switch (SW) and are converted into C-band again by

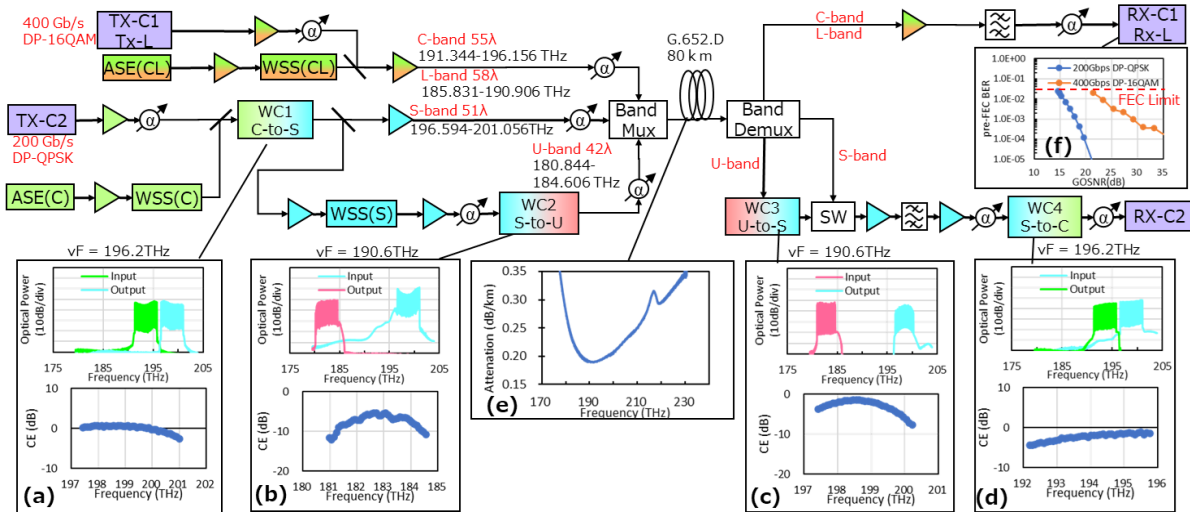


Fig. 2. Experimental setup of quad-band WDM transmission with PPLN-based wavelength converters WC1-WC4; (a) - (d) optical spectra of input and output signal, and CE of WC1-WC4, (e) characteristics of fiber attenuation, and (f) OSNR versus pre-FEC BER of transceiver

WC4. Figure 2 (f) shows the back-to-back GOSNR versus pre-FEC BER curves for each 400 Gb/s DP-16QAM and 200 Gb/s DP-QPSK signal at a signal frequency of 193.925 THz.

In this setup, 80-km SSMF transmission of quad-band WDM signals was carried out, and some test signals of each band were evaluated under 2 input power cases. Case 1 was set at -6 dBm/channel for each band in which the linear region was estimated, and case 2 was set at +2 dBm/channel for S-, C-, and L-band and -2 dBm/channel for U-band in which the nonlinear region was expected. U-band has an upper input power limit due to the CE of WC2. The transmission evaluation was measured by counting the pre-FEC BER and the uncorrected errors in the digital signal processing of the receiver. The converted GOSNR of each test channel measured pre-FEC BER is shown as a dot in Fig. 3, and calculated GOSNR from GSNR is shown as line in Fig.3. Note that the frequency range of test channel for L-band transceiver is 186.575 - 190.863 THz. In case 1, all S-, C-, L-band measured test channels are error-free, but almost U-band test channel are not error-free. The difference between the converted GOSNR and the calculated GOSNR was within 2.5 dB in all measured test channels. The main difference in GOSNR between the S-band and U-band is considered the effect of SNR<sub>NL</sub> of WC2. In case 2, ISRS generation and GOSNR improvement were confirmed by increasing fiber input power. All S-, C-, L-band test channels were error-free, and most of U-band test channels were error-free with equivalent to 3.412 THz. These results indicate that 80-km can be transmitted with a bandwidth corresponding to 17-THz, which is the sum of the bandwidth of the S-, C-, L-, and U-band measurable test channels. The difference between the converted GOSNR and the calculated GOSNR was within 3.3 dB in all measured test channels. In each band, a tendency to increase the error at the edge of the band was confirmed, and it is considered that there is a device which does not fully consider the wavelength dependence of SNR. However, the error was within 2 dB at center frequencies in each band, indicating that bandwidth extension to U-band can be investigated by incorporating a wavelength converter into GN model.

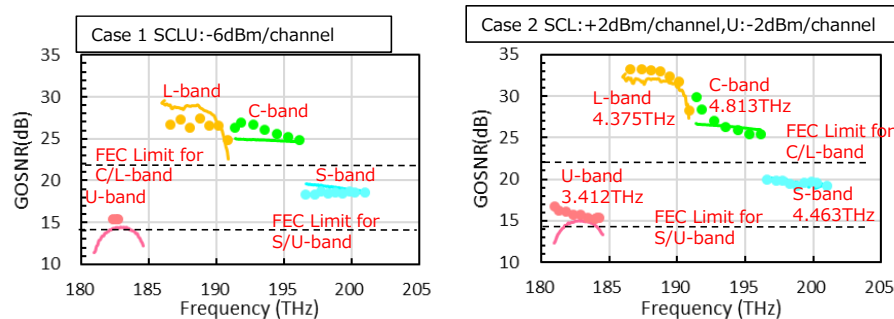


Fig. 3 GOSNR of 400-Gb/s DP-16QAM signal in C-/L-band and 200-Gb/s DP-QPSK signal in S-/U-band, dot: converted GOSNR from measured pre-FEC BER, line: calculated GOSNR from GSNR

#### 4. Conclusions

We demonstrated that over 17-THz S+C+L+U quadrable-band 80-km single-span transmission using C+L-band transceivers and PPLN-based wavelength converters. And we validated the mean absolute errors of the estimated pre-FEC BER based on GSNR from each linear SNR and nonlinear SNR were less than 3-dB compared to measured pre-FEC BER. By using wavelength converters, it is clarified that GN model-based channel power optimization can be applied to quadrable-band transmission including U-band. In the future, it is expected that the transmission distance and bandwidth will be expanded by carrying out the optimization of input power after investigating wavelength dependence of SNR in order to improve accuracy.

#### 5. Acknowledgement

This paper is partly based on results obtained from two projects carried out by Fujitsu Limited, JPNP20017, commissioned by the New Energy and Industrial Technology Development Organization (NEDO) and #04501, commissioned by the National Institute of Information and Communications Technology (NICT).

#### 6. References

- [1] F. Hamaoka et al., in JLT, vol. 37, no. 8, pp. 1764-1771, 2019.
- [2] T. Kato et al., in Proc. ECOC2019, PD.1.7, 2019.
- [3] S. Escobar-Landero et al., in Proc. OFC2023, Th3F.4, 2023.
- [4] T. Kato, et al., in PTL, in press.
- [5] M. Abe, et al., in Proc. FiO+LS2023, FM5D.2, 2023.
- [6] D. Soma, et al., in Proc. ECOC2023, Th.C.2.2, 2023.
- [7] B. Puttnam, et al., in Proc. ECOC2023, Th.C.2.4, 2023.
- [8] D. Semrau, et al., in JLT, vol. 37, no. 9, pp. 1924-1936, 2019.
- [9] Y. Jiang, et al., in Proc. ECOC2023, We.C.2.2, 2023.
- [10] K. Kimura, et al., in Proc. ECOC2023, We.C.2.3, 2023.
- [11] T. Kato, et al., in Proc. ECOC2022, We4D.4, 2022.
- [12] S. Shimizu, et al., in Proc. OFC2023, Th3F.3, 2023.